Assessment of Mouse VEGF Neutralization by Ranibizumab and Aflibercept

Yusuke Ichiyama (ichiyama@belle.shiga-med.ac.jp)
Shiga University of Medical Science
Riko Matsumoto
Shiga University of Medical Science
Shumpei Obata
Shiga University of Medical Science
Osamu Sawada
Shiga University of Medical Science
Yoshitsugu Saishin
Shiga University of Medical Science
Masashi Kakinoki
Shiga University of Medical Science
Tomoko Sawada
Shiga University of Medical Science
Masahito Ohji
Shiga University of Medical Science

Research Article

Keywords: Ranibizumab, aflibercept, mouse, murine, vascular endothelial growth factor

Posted Date: October 22nd, 2021

DOI: https://doi.org/10.21203/rs.3.rs-955481/v1

Abstract

There are many articles using bevacizumab, ranibizumab, and aflibercept as effective anti-vascular endothelial growth factor (VEGF) drugs in mice. However, it has been reported that bevacizumab lacks the ability to neutralize mouse VEGF. Here, we assessed the interaction between ranibizumab or aflibercept and mouse VEGF, both in vitro and in vivo. In vitro, we analyzed the interaction of mouse VEGF-A with aflibercept or ranibizumab as the primary antibody by Western blot, and observed immunoreactive bands for mouse VEGF-A in the aflibercept-probed blot, but not in the ranibizumab-probed blot. In vivo, we assessed the effect of intravitreal injection of ranibizumab and aflibercept on oxygen induced retinopathy and the effect of multiple intraperitoneal injections of ranibizumab and aflibercept on neonatal mice, and found that anti-VEGF effects were observed with aflibercept, but not with ranibizumab in both experiments. Our results suggest that aflibercept but not ranibizumab interacts with mouse VEGF. When conducting experiments using anti-VEGF drugs in mice, aflibercept is suitable, but ranibizumab is not.

Introduction

Intravitreal anti-VEGF injection has been a first line choice for the treatment of major retinal vascular diseases including age-related macular degeneration,[1–3] diabetic macular edema,[4,5] macular edema due to retinal vein occlusion,[6–8] myopic choroidal neovascularization,[9] and retinopathy of prematurity.[10,11] Currently, bevacizumab, ranibizumab, and aflibercept are the major anti-VEGF drugs in ophthalmic practice.[12] Accordingly, bevacizumab,[13–16] ranibizumab,[17–23] and aflibercept[24–28] are frequently used in experiments with mouse models of retinal vascular diseases. Notably, Ferrara N et al. reported that bevacizumab's ability to neutralize VEGF was species specific and lacking in mice.[29,30] It indicates that some types of anti-human VEGF antibody may be unsuitable for experiments in mice. Ranibizumab, a humanized monoclonal antibody Fab fragment, has the same structure as bevacizumab Fab except for five amino acids although ranibizumab and bevacizumab were generated from different anti-VEGF Fab fragments.[31] Aflibercept is a recombinant fusion protein, and its VEGF-binding portion consists of the extracellular domains from "human" VEGF receptors 1 and 2.[32] Therefore, it is possible that ranibizumab and aflibercept may lack the ability to neutralize mouse VEGF as bevacizumab. To the best of our knowledge, however, there is no report focusing on the interaction between ranibizumab or aflibercept and mouse VEGF. The purpose of this study is to assess the interactions of mouse VEGF with ranibizumab or aflibercept, both in vitro and in vivo.

Materials And Methods

Western blot analysis

The constituent proteins in 100, 50, or 25 ng of *Spodoptera frugiperda* insect cell (Sf 21)-derived recombinant human VEGF protein (165-amino acid isoform; R&D Systems, Inc., Minneapolis, MN, USA) or Sf 21-derived recombinant mouse VEGF (164-amino acid isoform; R&D Systems, Inc) were separated by SDS-PAGE and transferred to polyvinylidene difluoride membranes (Bio-Rad Laboratories, Inc., Hercules,

CA, USA). After blocking by 5% skim milk, the blots were incubated with aflibercept or ranibizumab at a final concentration of 1 μg/mL followed by anti-human IgG polyclonal antibody conjugated with horseradish peroxidase (for aflibercept) or an anti-human IgG F(ab')2 fragment-specific polyclonal antibody conjugated with horseradish peroxidase (for ranibizumab). Horseradish peroxidase activity was visualized using an enhanced chemiluminescence (ECL) detection system (FUJIFILM Wako Pure Chemical Corporation, Osaka, Japan).

Mice and tissue collection

All animal experiments were performed using C57BL/6J mice, their use for experimental purposes was approved by the Research Center for Life Sciences, Shiga University of Medical Science, and animal care was provided in accordance with institutional guidelines. All animal procedure were performed in compliance with the ARRIVE guidelines and were also carried out in accordance with the ARVO Statement for the Use of Animals in Ophthalmic and Vision Research. Before tissue sample removal and dissection, pups were anesthetized by isoflurane. After opening the thoracic cavity and exposing the heart, the right atrium was pierced and 5 mL of phosphate-buffered saline solution (PBS) was perfused through the left ventricle. Right after, 5 mL of 4% paraformaldehyde (PFA) at 4 °C was perfused in the same manner to start fixation of the tissues.

Oxygen induced retinopathy model and intraocular injection

An oxygen induced retinopathy (OIR) model using C57BL/6J mouse neonates was produced as previously described.[28] Briefly, at postnatal day (P) 8, mice with nursing mothers were exposed to 85% oxygen for 3 consecutive days. At P11, the mice were removed from the oxygen chamber and returned to room air. Intraocular injections of 0.5 μL of PBS, 20 μg of aflibercept (0.5 μL of Eylea®, Bayer AG, Leverkusen, Germany) or 5 μg of ranibizumab (0.5 μL of Lucentis®, Novartis Pharma K.K., Tokyo, Japan) into the vitreous body were performed at P12 using 33-gauge needles (ITO Corporation, Tokyo, Japan). Two days after injection (at P14), the eyes were harvested.

Multiple intraperitoneal injections in neonatal mice

PBS, 10 mg/kg of aflibercept, or 2.5 mg/kg or 10 mg/kg of ranibizumab was intraperitoneally injected into C57BL/6J mouse neonates daily from P3 to P6. The mice were weighed at all time points of injection. At P6, eyes and kidneys were harvested 6 hours after the last injection.

Immunohistochemistry

Whole-mounted retinas and pupillary membranes were produced according to previous reports.[28,38] Enucleated eyes were fixed for 30 minutes in 4% PFA at room temperature. A small hole was made in the cornea using a 27-gauge needle, and a circular incision was made using fine scissors. Then, retinal cups and pupillary membranes were dissected from the eyes and postfixed for 30 minutes in 4% PFA at 4°C.

Kidneys were fixed overnight in 4% PFA, snap-frozen in optimal cutting temperature (OCT) compound (Sakura Finetek USA, Inc., Torrance, CA, USA), and sectioned to a thickness of 12 μm.

The primary antibodies were biotinylated isolectin B4 (iB4, B-1205; 1:500; Vector Laboratories Inc., Burlingame, CA, USA), anti-CD31 (ab119341; 1:1000; Abcam plc, Cambridge, UK), anti-Ter119 (MAB1125; 1:250; R&D Systems, Inc.), anti-collagen IV (2150-1470; 1:500; Bio-Rad Laboratories, Inc.), and anti-Erg (ab92513; 1:2000; Abcam plc, Cambridge, UK). The secondary antibodies were suitable species-specific secondary antibodies (Jackson ImmunoResearch Laboratories, Inc., West Grove, PA, USA) or streptavidin coupled to Alexa Fluor dyes (Invitrogen, Waltham, MA, USA). For nuclear staining, specimens were treated with DAPI (Santa Cruz Biotechnology, Inc., Dallas, TX, USA).

Proliferation assay in vivo

For in vivo analysis of cell proliferation, 5 μg of 5-ethynyl-2-deoxyuridine (EdU, C10337; Invitrogen) per gram of body weight was injected intraperitoneally 2 hours before sacrifice. Retinas were dissected and immunostained as described above. After secondary antibody staining, EdU labeling was detected by means of a Click-it EdU Alexa Fluor-488 Imaging Kit (C10337; Invitrogen) according to the manufacturer's instructions.

Image acquisition and quantification

All fluorescence images were obtained using a confocal laser-scanning microscope (Leica TCS SP8, Leica Microsystems GmbH, Wetzlar, Germany). The image-based quantification methods are described in previous reports.[28,38,39] The ratio of the avascular area to the whole retinal area (% avascular area), the ratio of the neovascular tufts area to the whole retinal area (% NVT area), the ratio of the $Ter119^+$ area to the whole retinal area (% $Ter119^+$ area), the distance from the optic disc to the vascular front (radial growth), and total pupillary vessel length were measured manually using image J software. The sinuosity index of retinal vessels was calculated using the following formula: The sinuosity index = total curvilinear length of retinal vessels / total Euclidean distance between vascular branching points. The vessel density was calculated by using a binarization method. The $colIV^+CD31^-$ area was considered as the area of regressed capillaries according to previous reports,[34,35] and the ratio of the $colIV^+CD31^-$ area to the total $colIV^+$ area (% area of regressed capillaries) was calculated. To quantify the number of endothelial cells (ECs), the EC-specific nuclear marker (Erg) was used and EdU^+Erg^+ cells were considered to be proliferating ECs.[36]

Statistical analysis

All statistical analyses were conducted using SPSS statistics (version 22; International Business Machines Co. Limited, New York, NY, USA). One-way analysis of variance was used for comparison between independent groups. A value of $P<0.05$ was considered statistically significant.

Results

No binding of ranibizumab to mouse VEGF-A in vitro

Western blot analysis of the binding of human and mouse VEGF-A with aflibercept or ranibizumab as the primary antibody is shown in Fig. 1. In the aflibercept-probed blot, immunoreactive bands of the expected size for both human and mouse VEGF-A were observed. On the other hand, in the ranibizumab-probed blot, immunoreactive bands were observed for human VEGF-A, but not for mouse VEGF-A even with long exposure time (10 min).

No effect of intravitreal ranibizumab injection in OIR mice

To evaluate the neutralization of mouse VEGF by aflibercept and ranibizumab in vivo, we examined retinal vascular structural changes after intravitreal injection of aflibercept and ranibizumab in oxygen-induced-retinopathy (OIR) model mice (Fig. 2). When compared to PBS injected eyes, aflibercept injected eyes showed neovascular tufts (NVT) area reduction (P=0.02, Fig. 2C), avascular area enlargement (P<0.01, Fig. 2D), and decreased sinuosity of retinal vessels (P<0.01, Fig. 2E). In ranibizumab injected eyes, however, the NVT area (P=1.00, Fig. 2C), avascular area (P=0.97, Fig. 2D), and sinuosity of retinal vessels (P=0.92, Fig. 2E) were comparable with those of PBS injected eyes.

No effect of multiple intraperitoneal ranibizumab injections in neonatal mice

As described above, no retinal vascular change was observed after a single intravitreal ranibizumab injection in the analysis using OIR model mice. However, some neutralization of mouse VEGF might be observed by increasing the dose or frequency of ranibizumab administration. Since it is difficult to administer a large amount of drug or multiple doses of drug via intravitreal injection, we conducted the examination using multiple intraperitoneal injection of a large amount of anti-VEGF drugs in neonatal mice (Fig. 3A).

After 4 intraperitoneal injections of PBS, aflibercept (10 mg/kg), or a low (2.5 mg/kg) or high (10 mg/kg) dose of ranibizumab, body weight gain in pups treated with aflibercept was significantly impaired comparing with other three groups (P<0.01, Fig. 3B). The body weight gain in pups treated with 2.5 mg/kg or 10 mg/kg of ranibizumab was comparable with that in PBS treated pups (P=0.99). The whole-mounted retinas in the aflibercept group also showed apparent retinal hemorrhage (arrowheads in Fig. 3C), increased $Ter119^+$ area (P=0.04, Fig. 3D), retinal vascular growth impairment (P=0.04, Fig. 3C, E), decreased number of branching points (P<0.01, Fig. 3F, G), increased area of $colIV^+CD31^-$ regressed capillaries (P<0.01, filled arrowheads in Fig. 3F, H), and decreased number of EdU^+Erg^+ proliferating ECs (P<0.01, open arrowheads in Fig. 3F, I), in contrast to the ranibizumab groups. Furthermore, decreased pupillary vessel length (P<0.01, Fig. 3J, K) and density (P<0.01, Fig. 3J, L), pathological renal thrombosis (arrowheads in Fig. 3M), decreased renal vessel density (P<0.01, Fig. 3M, N), and decreased number of glomerular ECs (P<0.01, Fig. 3M, O) were observed in the aflibercept group, but not in the ranibizumab groups.

Discussion

Both in vitro and in vivo, we did not observe any interaction between ranibizumab and mouse VEGF-A. This is a reasonable result because the structure of ranibizumab is similar to that of bevacizumab Fab, which lacks the ability to interact with mouse VEGF.[29,30] Since there are many articles about the use of ranibizumab as an effective anti-VEGF drug in mice,[17-23] we believe it is necessary to alert ophthalmology researchers against using ranibizumab as an anti-VEGF drug in the future mouse experiments.

It is unclear why ranibizumab showed anti-VEGF effects in previous reports,[17-22] but we suspect that the use of poor quantitative methods such as fluorescein angiography,[19] immunostaining of retinal sections,[18-20] or fluorescein isothiocyanate (FITC)-dextran perfused retinal flat mounts[18,20] may have led to different results. Fluorescein angiography is suitable for qualitative analysis, but not quantitative analysis because the amount of flash light and the timing of the photography after fluorescein injection may cause the results to vary. Immunostaining of retinal sections is also not suitable for quantitative analysis, especially in retinal vessels, because the quantitative results greatly depend on the slice position. FITC-dextran perfused retinal flat mounts have the following weakness: if the perfusion of FITC-dextran injected into the heart is inadequate, neovascular area may be underestimated and avascular area overestimated. Unlike these methods, immunostaining of whole-mounted retina is suitable for quantitative analysis because the entire retinal vascular structure can be observed clearly.[28,33-36] In this study, we analyzed high quality images of whole-mounted retina and found ranibizumab had no effect on retinal vessels. From this fact and the fact that ranibizumab did not bind to mouse VEGF in vitro experiments, we conclude that ranibizumab has no neutralizing effect on mouse VEGF.

In the in vivo experiments of this study, we first analyzed change in retinal vascular structure after intravitreal injection of anti-VEGF drugs using OIR mice and found no anti-VEGF effect of ranibizumab in OIR retina. In this method using OIR model mice, however, small anti-VEGF effects may be missed because of a large variation in the degree of retinopathy between individual OIR model mice and because of the dosage limit in ocular administration. In order to capture even a small anti-VEGF effect, we conducted an additional experiment in which an extremely large dose of anti-VEGF drug was administered intraperitoneally to neonatal mice because there is little variation in vascular development between individual neonatal mice. In this additional experiment, we administered 10 mg/kg (87 nmol/kg) of aflibercept, or 2.5 mg/kg (52 nmol/kg) or 10 mg/kg (208 nmol/kg) of ranibizumab for 4 consecutive days, which are much higher doses than the dose of aflibercept used as an anti-cancer drug in humans (35 nmol/kg every two weeks). However, multiple administration of extremely large doses of ranibizumab to neonatal mice did not cause any change compared to PBS administration. Although our results could be influenced by the difference in the clearance rate from the circulation between ranibizumab and aflibercept,[37] we believe our results still suggest that ranibizumab does not neutralize mouse VEGF.

In conclusion, ranibizumab does not neutralize mouse VEGF, both in vivo and in vitro. When conducting experiments using anti-VEGF drugs in mice, aflibercept is suitable, but ranibizumab is not.

Declarations

Acknowledgments

We thank Fumiko Kimura for her technical support.

This work was supported by grants-in-aid for Scientific Research on Innovative Areas from the Ministry of Education, Culture, Sports, Science, and Technology of Japan (19K18877). This funding organization had no role in the design or conduct of this study.

Conflict of interest statement

The authors have no conflicts of interest to declare.

Author contributions

Y. Ichiyama and M. Ohji designed research; Y. Ichiyama and R. Matsumoto performed research; Y. Ichiyama, S. Obata, O. Sawada, Y. Saishin, M. Kakinoki, and T. Sawada analyzed data; Y. Ichiyama and M. Ohji wrote the paper.

References

1. Brown, D. M. *et al.* Ranibizumab versus verteporfin for neovascular agerelated macular degeneration. *N Engl J Med*, **355**, 1432–1444 (2006).
2. CATT Research Group. et al. Ranibizumab and bevacizumab for neovascular agerelated macular degeneration. *N Engl J Med*, **364**, 1897–1908 (2011).
3. Heier, J. S. *et al.* Intravitreal aflibercept (VEGF trap-eye) in wet age-related macular degeneration. *Ophthalmology*, **119**, 2537–2548 (2012).
4. Diabetic Retinopathy Clinical Research Network. et al. Aflibercept, bevacizumab, or ranibizumab for diabetic macular edema. *N Engl J Med*, **372**, 1193–1203 (2015).
5. Jampol, L. M., Glassman, A. R. & Sun, J. Evaluation and Care of Patients with Diabetic Retinopathy. *N Engl J Med*, **382**, 1629–1637 (2020).
6. Campochiaro, P. A. *et al.* Ranibizumab for macular edema following branch retinal vein occlusion: six-month primary end point results of a phase III study. *Ophthalmology*, **117**, 1102–1112 (2010).
7. Brown, D. M. *et al.* Ranibizumab for macular edema following central retinal vein occlusion: six-month primary end point results of a phase III study. *Ophthalmology*, **117**, 1124–1133 (2010).
8. Scott, I. U., Campochiaro, P. A., Newman, N. J. & Biousse, V. Retinal vascular occlusions. *Lancet*, **396**, 1927–1940 (2020).
9. Cheung, C. M. G. *et al.* Myopic Choroidal Neovascularization: Review, Guidance, and Consensus Statement on Management. *Ophthalmology*, **124**, 1690–1711 (2017).

10. Mintz-Hittner, H. A., Kennedy, K. A., Chuang, A. Z. & BEAT-ROP Cooperative Group. Efficacy of intravitreal bevacizumab for stage 3+ retinopathy of prematurity. *N Engl J Med*, **364**, 603–615 (2011).
11. Stahl, A. *et al.* Ranibizumab versus laser therapy for the treatment of very low birthweight infants with retinopathy of prematurity (RAINBOW): an open-label randomised controlled trial. *Lancet*, **394**, 1551–1559 (2019).
12. Ferrara, N. & Adamis, A. P. Ten years of anti-vascular endothelial growth factor therapy. *Nat Rev Drug Discov*, **15**, 385–403 (2016).
13. Bock, F. *et al.* Bevacizumab as a potent inhibitor of inflammatory corneal angiogenesis and lymphangiogenesis. *Invest Ophthalmol Vis Sci*, **48**, 2545–2552 (2007).
14. Rabinowitz, R., Priel, A., Rosner, M., Pri-Chen, S. & Spierer, A. Avastin treatment reduces retinal neovascularization in a mouse model of retinopathy of prematurity. *Curr Eye Res*, **37**, 624–629 (2012).
15. Akkoyun, I. *et al.* Structural consequences after intravitreal bevacizumab injection without increasing apoptotic cell death in a retinopathy of prematurity mouse model. *Acta Ophthalmol*, **90**, 564–570 (2012).
16. Feng, F., Cheng, Y. & Liu, Q. H. Bevacizumab treatment reduces retinal neovascularization in a mouse model of retinopathy of prematurity. *Int J Ophthalmol*, **7**, 608–613 (2014).
17. Bucher, F. *et al.* Topical Ranibizumab inhibits inflammatory corneal hem- and lymphangiogenesis. *Acta Ophthalmol*, **92**, 143–148 (2014).
18. Jiang, C., Ruan, L., Zhang, J. & Huang, X. Inhibitory effects on retinal neovascularization by ranibizumab and sTie2-Fc in an oxygen-induced retinopathy mouse model. *Curr Eye Res*, **43**, 1190–1198 (2018).
19. Yan, Z. *et al.* Inhibition of YAP ameliorates choroidal neovascularization via inhibiting endothelial cell proliferation. *Mol Vis*, **24**, 83–93 (2018).
20. Li, W. *et al.* Soluble Tei2 fusion protein inhibits retinopathy of prematurity occurrence via regulation of the Ang/Tie2 pathway. *Exp Ther Med*, **18**, 614–620 (2019).
21. Chen, W. *et al.* Role of TLR4-MAP4K4 signaling pathway in models of oxygen-induced retinopathy. *FASEB J*, **33**, 3451–3464 (2019).
22. Xie, F. *et al.* Notch signaling pathway is involved in bFGF-induced corneal lymphangiogenesis and hemangiogenesis. J Ophthalmol 2019, 9613923 (2019).
23. Zhong, D. J. *et al.* Adenosine A 2A receptor antagonism protects against hyperoxia-induced retinal vascular loss via cellular proliferation. *FASEB J*, **35**, e21842 (2021).
24. Saishin, Y. *et al.* VEGF-TRAP(R1R2) suppresses choroidal neovascularization and VEGF-induced breakdown of the blood-retinal barrier. *J Cell Physiol*, **195**, 241–248 (2003).
25. Tokunaga, C. C. *et al.* Effects of anti-VEGF treatment on the recovery of the developing retina following oxygen-induced retinopathy. *Invest Ophthalmol Vis Sci*, **55**, 1884–1892 (2014).

26. Tang, F. *et al.* Anti-secretogranin III therapy of oxygen-induced retinopathy with optimal safety. *Angiogenesis*, **22**, 369–382 (2019).
27. Amin, S. M. *et al.* Efficacy of Aflibercept Treatment and Its Effect on the Retinal Perfusion in the Oxygen-Induced Retinopathy Mouse Model of Retinopathy of Prematurity. *Ophthalmic Res*, **64**, 91–98 (2020).
28. Ichiyama, Y. *et al.* The systemic antiangiogenic effect of intravitreal aflibercept injection in a mouse model of retinopathy of prematurity. *FASEB J*, **35**, e21390 (2021).
29. Ferrara, N., Hillan, K. J., Gerber, H. P. & Novotny, W. Discovery and development of bevacizumab, an anti-VEGF antibody for treating cancer. *Nat Rev Drug Discov*, **3**, 391–400 (2004).
30. Yu, L. *et al.* Interaction between bevacizumab and murine VEGF-A: a reassessment. *Invest Ophthalmol Vis Sci*, **49**, 522–527 (2008).
31. Ferrara, N., Damico, L., Shams, N., Lowman, H. & Kim, R. Development of ranibizumab, an anti-vascular endothelial growth factor antigen binding fragment, as therapy for neovascular age-related macular degeneration. *Retina*, **26**, 859–870 (2006).
32. Holash, J. *et al.* VEGF-Trap: a VEGF blocker with potent antitumor effects. *Proc Natl Acad Sci USA*, **99**, 11393–11398 (2002).
33. Okabe, K. *et al.* Neurons limit angiogenesis by titrating VEGF in retina. *Cell*, **159**, 584–596 (2014).
34. Baffert, F. *et al.* Cellular changes in normal blood capillaries undergoing regression after inhibition of VEGF signaling. *Am J Physiol Heart Circ Physiol*, **290**, H547–59 (2006).
35. Mancuso, M. R. *et al.* Rapid vascular regrowth in tumors after reversal of VEGF inhibition. *J Clin Invest*, **116**, 2610–2621 (2006).
36. Eilken, H. M. *et al.* Pericytes regulate VEGF-induced endothelial sprouting through VEGFR1. *Nat Commun*, **8**, 1574 (2017).
37. Liming, L. Pharmacokinetics of monoclonal antibodies and Fc-fusion proteins. *Protein Cell*, **9**, 15–32 (2018).
38. Takahashi, M. *et al.* Macrophages fine-tune pupil shape during development. *Dev Biol*, **464**, 137–144 (2020).
39. Ichiyama, Y., Sawada, T., Ito, Y., Kakinoki, M. & Ohji, M. Optical coherence tomography angiography reveals blood flow in choroidal neovascular membrane in remission phase of neovascular age-related macular degeneration. *Retina*, **37**, 724–730 (2017).

Figures

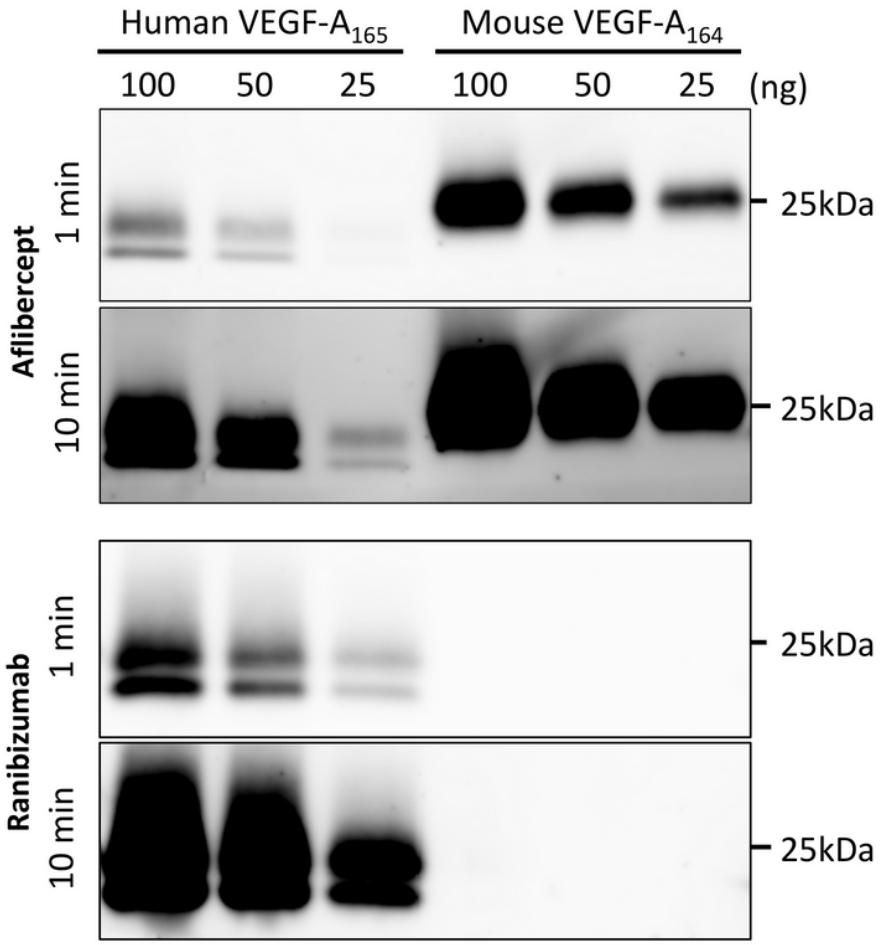

Figure 1

Western blot analysis of the interaction of recombinant human VEGF-A165 and mouse VEGF-A164 with aflibercept or ranibizumab as the primary antibody. The immunoreactive bands for mouse VEGF-A were observed in the aflibercept-probed blot, but not in the ranibizumab-probed blot even with long exposure time. The full-length blots are presented in Supplementary Figure S1. VEGF, vascular endothelial growth factor.

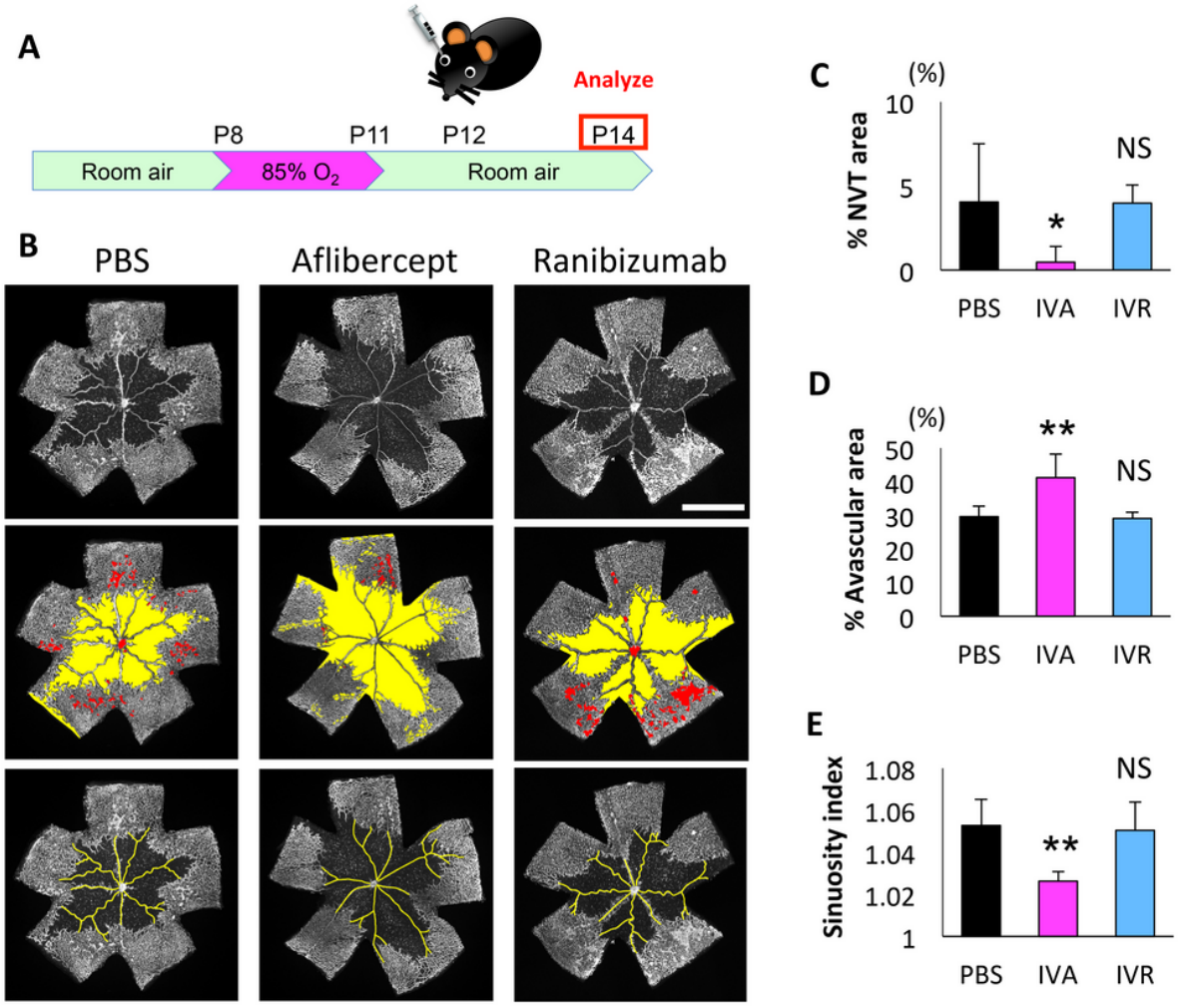

Figure 2

The effect of intravitreal injection of ranibizumab and aflibercept on oxygen induced retinopathy. (A) A schematic diagram depicting the time course of our experiment. (B) Whole-mounted stained retinas on day 2 after injection. (C) The reduction of the NVT area was observed in aflibercept injected eyes, but not in ranibizumab injected eyes. (C) Avascular area enlargement was observed in aflibercept injected eyes, but not in ranibizumab injected eyes. (E) Decreased sinuosity of the retinal vessel was observed in aflibercept injected eyes, but not in ranibizumab injected eyes. Scale bars represent 1000 μm; **P<0.01; *P<0.05 (n=7 /group). Data are presented as mean ± SD. PBS, phosphate-buffered saline solution; IVA, intravitreal aflibercept; IVR, intravitreal ranibizumab; NVT, neovascular tuft; NS, not significant.

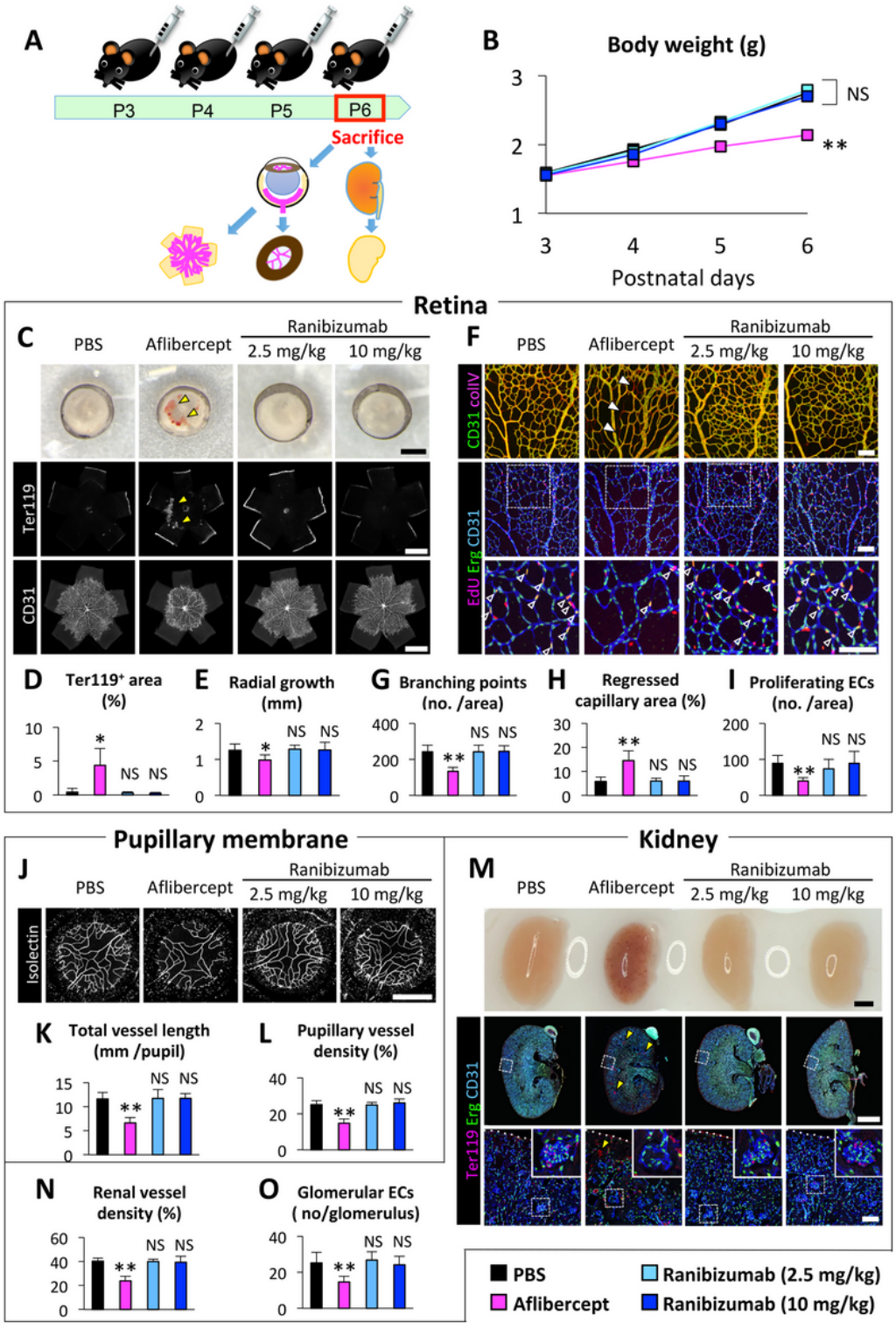

Figure 3

The effect of ranibizumab and aflibercept injected intraperitoneally into neonatal mice. (A) A schematic diagram depicting the time course of our experiment. (B) The body weight gains were impaired in the aflibercept group but not in the ranibizumab groups. (C-E) The whole-mounted retinas showed apparent retinal hemorrhage (arrowheads) and vascular growth impairment in the aflibercept group but not in the ranibizumab groups. (F-I) The high magnification images of the whole-mounted retinas show decreased

number of branching points, increased area of regressed capillaries (filled arrowheads), and decreased number of proliferating ECs (open arrowheads) in the aflibercept group but not in the ranibizumab groups. (J-L) The whole-mounted pupillary membranes showed decreased pupillary vessel length and density in the aflibercept group but not in the ranibizumab groups. (M-O) The kidney sections showed pathological renal thrombosis (arrowheads), decreased density of renal vessels, and decreased number of glomerular endothelial cells in the aflibercept group but not in the ranibizumab groups. Scale bars represent 1000 μm (C, top and middle rows of M); 500 μm (J); 100 μm (F and bottom row of M); **P<0.01; *P<0.05 (n=6-7 /group). ECs, endothelial cells; NS, not significant; PBS, phosphate-buffered saline solution.

Supplementary Files

This is a list of supplementary files associated with this preprint. Click to download.

- FigureS1.tif